Duplex ball bearing outer ring deformation- Simulation and experiments

Mor Battat[1], Gideon Kogan[1], Alex Kushnirsky[1], Renata Klein[2] and Jacob Bortman[1]

[1]*Pearlstone Center for Aeronautical Engineering Studies and Laboratory for Mechanical Health Monitoring, Department of Mechanical Engineering, Ben-Gurion University of the Negev, P.O. Box 653, Beer Sheva 84105, Israel*

morbat@post.bgu.ac.il
jacbort@bgu.ac.il

[2]*R.K. Diagnostics, P.O.Box 101, Gilon, D. N. Misgav 20103, Israel*

Renata.Klein@rkdiagnostics.co.il

ABSTRACT

This paper presents a research of deformations influence on duplex ball bearings dynamic behavior. Despite the common use of duplex ball bearings, bearings sub-components deformations are not thoroughly investigated. In order to investigate these effects, this study integrates the outcome of a 3D dynamic model, developed for assessment of the defect pattern and experimental results from a full scale CH-53 Swashplate test rig.

The ability to withstand high radial and bi-directional axial loads makes duplex bearings common in aircraft applications and specifically in helicopter rotors. The swashplate of the CH-53 is constructed of duplex angular contact ball bearings. Two spacers, internal between the static inner rings and external, between the rotating outer rings support the bearing rings. A structural defect is formed by a faulty external spacer, thus causing a lack of support to the top bearing and deformation of the outer rings.

Model results indicate that the lack of support has a defect pattern in both radial and axial directions. Test rig data acquired by accelerometers was analyzed by several diagnostic techniques including order tracking, envelope analysis and dephased algorithm in order to recognize the simulated pattern.

1. INTRODUCTION

Duplex (paired) bearings are used in a wide range of applications. The ability to withstand high radial and bi-directional axial loads makes duplex bearings common in aviation applications, specifically in helicopter rotors.

The CH-53 swashplate is constructed of duplex angular contact ball bearings in a back-to-back arrangement (Figure 1). The bearings allow smooth relative motion between the static plate and a rotating plate while absorbing torques from the pitch control rods. The bearings are separated by two spacers, internal between the static inner rings and external between the rotating outer rings (Figure 2).

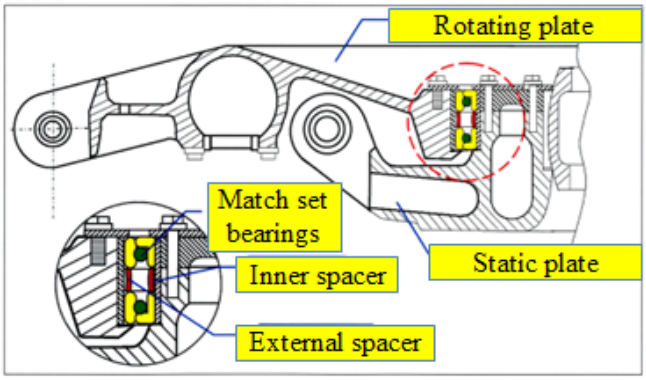

Figure 1. Cross section of a CH-53 Swashplate

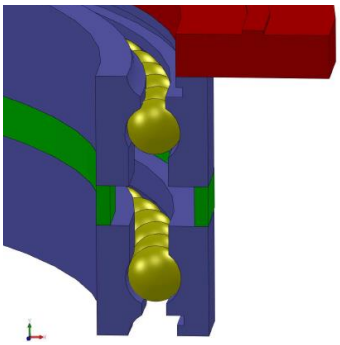

Figure 2. Magnified section of the angular-contact ball bearings and the spacers separating the rings

This study focuses on the recognition of deformation of the bearings outer rings caused by buckling of the external spacer. As shown in Figure 3, integration of dynamic model results and seeded test experiments serve as the methodology of the research. Time history data generated by the model was analyzed in order to define the fault expected pattern. Vibration signals generated by the experimental systems will be analyzed based on the model results in order to recognize the fault signature.

Development of diagnostic tools on a test stand is a complicated process due to environmental factors. These factors include structural dynamics, mounting, location, components history and reciprocal influence. This approach is designed to address the complexity of algorithms development based on test rig data. The integration of a physical model and hierarchical test systems is a method designed to assist in recognition of the fault pattern in the different experimental systems.

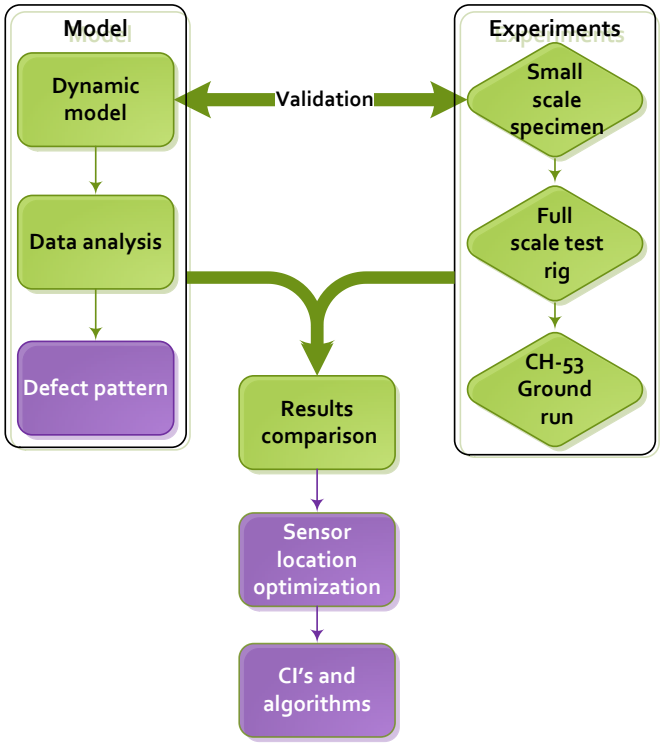

Figure 3. Research methodology- integration of model results and experiments at different scales

1.1. Research Background

A 3D dynamic model (Kogan et al., 2012) has been developed for assessment of the defect pattern and for comprehension of common effects such as radial load and misalignment. Time history data simulated by the model was analyzed in order to define the expected fault pattern.

Comparing the dynamic model results with vibration signals generated by different test systems is planned in phases. It is assumed that when advancing from one phase to another the measured data will simulate more realistically the signal and the environment of the helicopter rotor head. As a result, the difficulty to recognize the fault pattern is expected to increase from one phase to another, demanding more complex algorithms. Progress in phases is performed to guarantee the recognition of the defect signature among the variety of signals generated by the helicopter during a flight.

The experimental phases include a small scale specimen, full scale test rig and a CH-53 helicopter ground test. Further background of this work is presented in the paper (Battat at el., 2013) and includes description and results of the small scale specimen.

2. DYNAMIC MODEL

A 3D dynamic ball bearing model was developed by Kogan et al (2012) to study the effect of anomalies in bearing sub-components on the bearing dynamic behavior. The non-linear model was developed using Hertzian contact theory and has the ability to simulate effects of radial and axial loads, shaft unbalance, localized faults, and ring deformation. The algorithm was implemented numerically in MATLAB. Model validation by the small scale specimen was described in referenced work.

In order to simulate the bearings outer rings deformation, analytic approximation of the sagging was done. This approximation takes into account applied load, length of the defect, number of effected balls and structural parameters.

3. TEST RIG

In order to examine the effect of defects on the dynamic behavior of the CH-53 swashplate bearings, a specific test rig was constructed. The main purpose of the full scale test rig was to simulate the original work environment of the swashplate bearings without the environmental noise. The reduction of noise will help in recognition and isolation of the searched pattern.

The rig (Figure 4) is composed of an original CH-53 swashplate and provides a good simulation of the bearings support structure under laboratory conditions. The rotating plate is set in motion by a transmission of gears and a cog belt driven by an electric three phase motor. Controlled by a variable frequency drive, the motor is set to rotate the plate up to 189 RPM (3.15 Hz), the CH-53 main rotor speed. Table 1 lists the bearings parameters.

Table 1. Test rig bearings parameters

Pitch diameter	19.03 $[in]$
Ball diameter	0.5 $[in]$
Number of balls	92
Outer race rotational speed	189 $[rpm]$
Contact angle	30°
Defect angular length	68°

Figure 4. Full scale test rig and sensors locations

An aluminum external spacer separates the bearings outer rings. Unlike local defects, the buckling phenomenon is correlated with a relatively large length dimension. Hence, in order for the fault to be presented an arc length of nearly 70° was inserted to the external spacer. The defect is formed by milling both vertical ends of the spacer for a 300 mm arc (Figure 5). Milling the external spacer causes a lack of support to the bearings outer rings in the presence of axial load.

Simulation of the axial load on the swashplate is carried out using a hydraulic cylinder. By producing tension in the main shaft the piston loads the rotating plate, thus axially loading the bearing's outer rings. Figure 6 demonstrates the path of the load through the test rig.

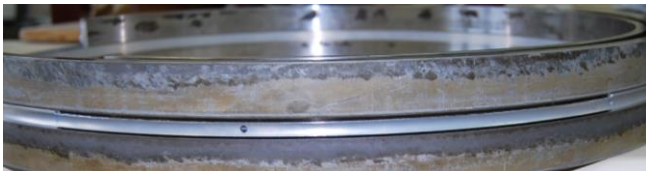

Figure 5. Faulty external spacer separating the bearings outer rings. Lack of support is simulated by milling the spacer's vertical ends.

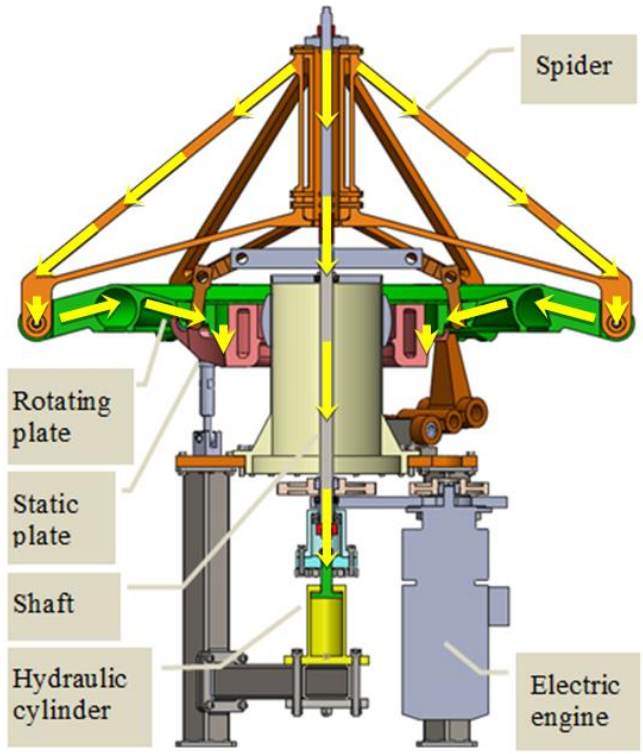

Figure 6. Load transformation over the test rig

The rotational speed of the plate is measured by a magnetic speed sensor. Vibration signals were collected by triaxial piezoelectric accelerometer positioned at several locations marked on Figure 4. The accelerometers are mounted with one of their axes parallel to the rigs axial axis (line of action). Data was collected in several rotational speeds and piston pressures in both healthy and faulty swashplates.

4. MODEL RESULTS

During a ball passage through the outer ring deflected zone, the load acting on the ball drops and the ball support of the outer ring is reduced. In order to compensate for the support reduction, the balls outside the deflected zone are overloaded. The interruption caused by interaction of a ball with the deflected zone causes a periodic impact.

Cycle domain of the simulated results is presented in Figure 7. The axial direction coincides with the bearing axis, while Radial 1 and Radial 2 are directions of measurement located in the bearing plane. Model results simulate a sensor located at the center of the inner ring. Since the defect location varies with the shaft rotation shaft speed modulation is created in the radial directions.

Further analysis was performed using Power spectral density (PSD). The spectrum of the axial acceleration reveals peaks at harmonics of the Outer race Ball Pass Frequency (BPFO). BPFO harmonics are presented in Figure 8 as the repetitive high peaks. The spectrum of the radial acceleration reveals peaks at shaft speed sideband around the BPFO harmonics (Figure 9). In order to obtain a closer to reality simulation, a small value radial load was inserted. This modification is expressed by an additional sideband.

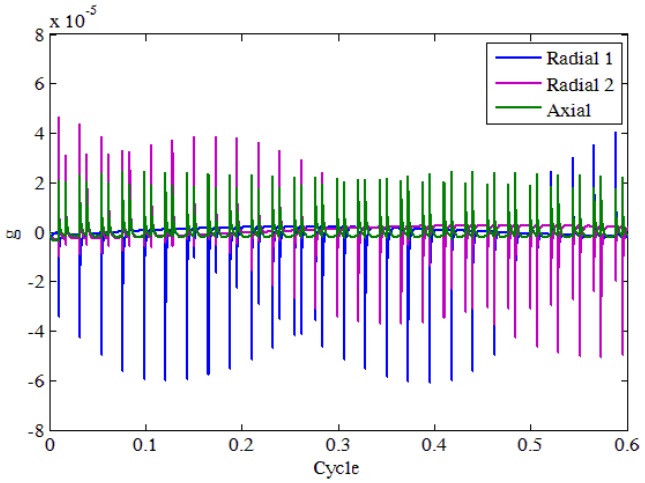

Figure 7. Simulated results: acceleration of the inner ring

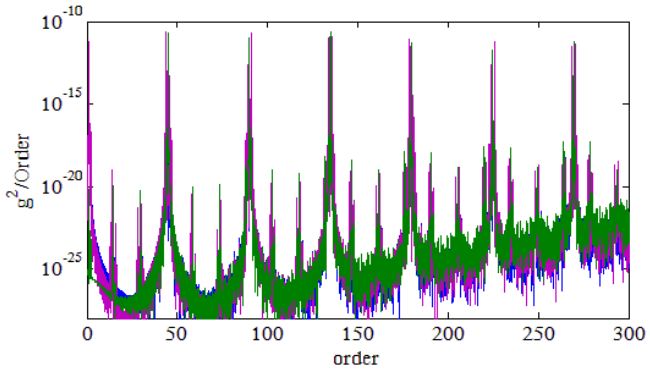

Figure 8. Simulated results: Order of a faulty duplex bearing under combined load. Axial, radial 1 and radial 2 are in green, blue and purple respectively

Model simulations present the defect signature as BPFO harmonies with adjacent shaft speed sidebands. The BPFO is calculated for 44.95 [$order$] and is clearly visible as the main peak in the axial direction. Background sidelobes are significantly lower than the radial sidebands and therefore are not part of the pattern. Following harmonics present a similar image. Therefore this pattern was used for comparison to BPFO harmonics of the experimental results.

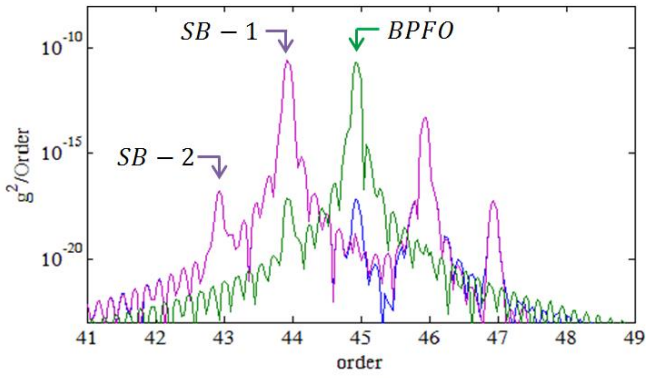

Figure 9. Simulated results: order of the BPFO first harmonic. Axial, radial 1 and radial 2 are in green, blue and purple respectively

5. EXPERIMENTAL RESULTS

Test rig results present a significantly more complex image. Vibration sensors are sensitive to data from a variety of elements in the system. In addition, effects of misalignment unbalance and transfer functions are present. Use of order tracking, envelope analysis and signal dephase are described in this section. These are applied in order to separate the fault pattern from the noisy environment.

Figure 10 presents the order representation (PSD of the resampled signal) of the measured signal of a piezoelectric tri-axial sensor mounted at location 1.

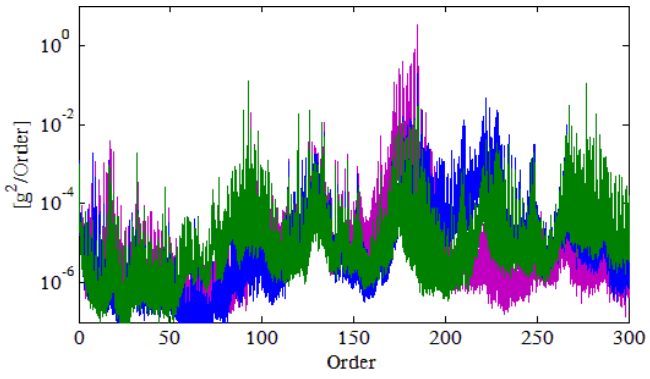

Figure 10. Measured data: Order representation of the tri-axial data at location 1. Axial, radial 1 and radial 2 are in green, blue and purple respectively

Data was acquired at various locations (marked on Figure 4). The data was examined and location 1 was selected as the bearing was most noticeable in its signals. Through examining the analyzed data, it was found that the BPFO order is estimated at 44.98 and the inner race Ball Pass Frequency (BPFI) order is estimated at 47.03. The proximity of the bearings tones to a harmonic of the shaft speed causes a difficulty in recognition of the bearing tone and its sidebands in the vicinity of the first harmonic (see Figure 11). This illustrates the difficulties in recognizing the pattern in a realistic environment. A clear image of the defect pattern is obtained at the BPFO 7th harmonic and is presented in Figure 12. Unlike the model results, both the PBFO harmony and the shaft speed sidebands are presented in all measuring directions. The main reason for this is inherent in the behavior of the transfer function and related to the proximity of the sensor to the bearing.

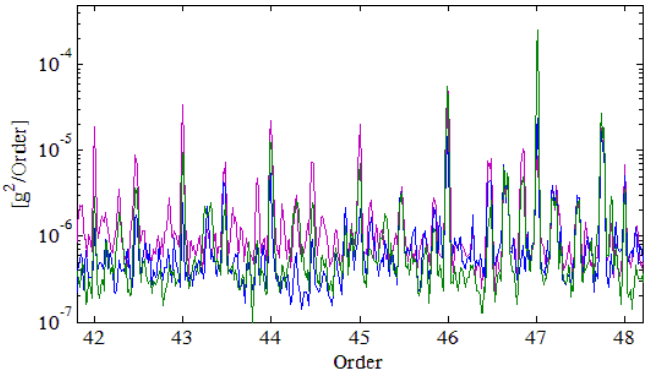

Figure 11. Measured data: Order of the BPFO first harmonic. Axial, radial 1 and radial 2 are in green, blue and purple respectively

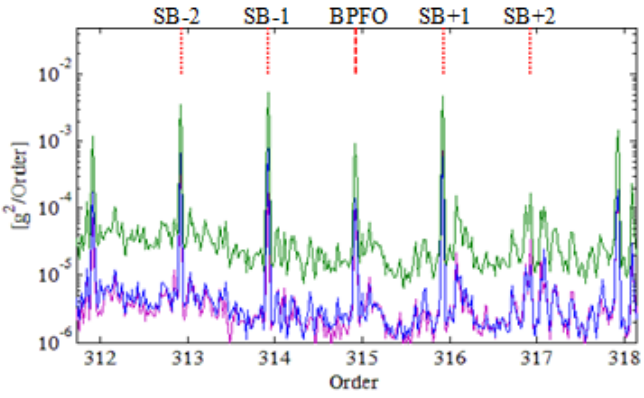

Figure 12. Measured data: Order of the BPFO 7th harmonic. Axial, radial 1 and radial 2 are in green, blue and purple respectively

5.1. Advanced analysis

An advanced analysis is used to identify the fault in noisy environment. The dephase algorithm (Klein et-al, 2012) attenuates peaks synchronous to the rotating speeds of shafts (gear mesh frequencies, shaft harmonics). By that, weak signals related to bearings that have been masked by other vibration sources might become visible. Figure 13 presents the dephased signal marked in green against the background of the order signal (in orange). The second BPFO harmonic was masked by the cog belt signal at order 90. Accordingly, BPFO sidebands are unrecognized without the dephased analysis. Figure 14 presents the dephased signal of the axial direction centered at the third BPFO harmonic.

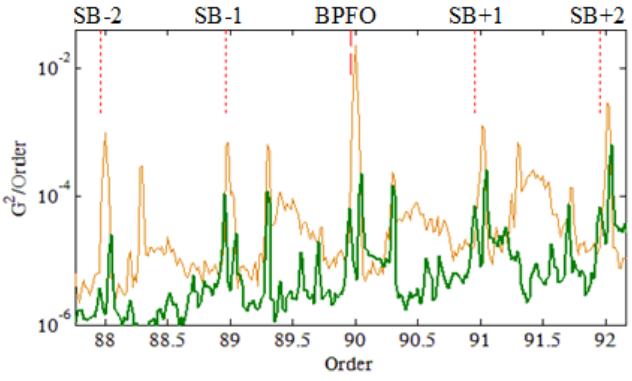

Figure 13.Measured data: axial direction of the second BPFO harmonic. Order of the dephased signal (green) against the background of the order signal (orange).

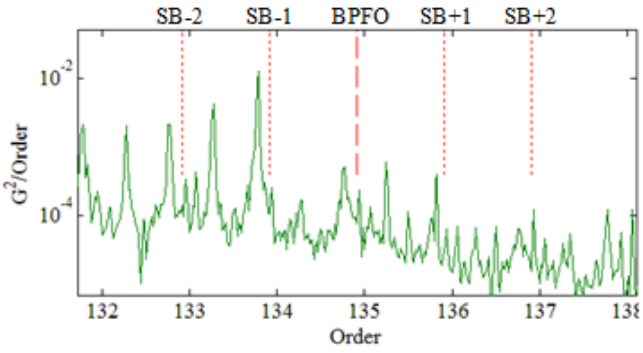

Figure 14. Measured data: Order of the dephased axial direction, third BPFO harmonic

Envelope analysis is a known technique for identification of bearing faults. The envelope signal was calculated based on the dephased signal and is presented in Figure 15 and Figure 16. The order representation of the envelope shows a clear bearing pattern and good agreement with the model results.

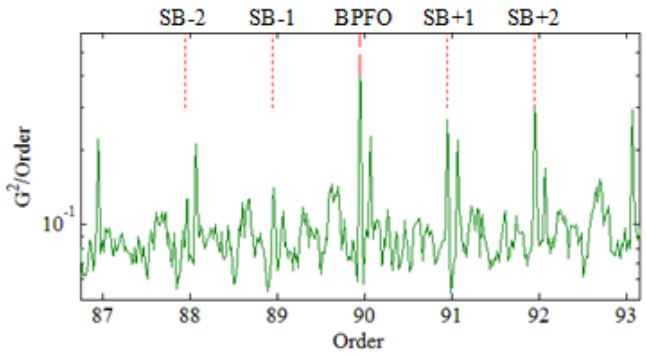

Figure 15. Measured data: Order of the envelope axial direction, second BPFO harmonic

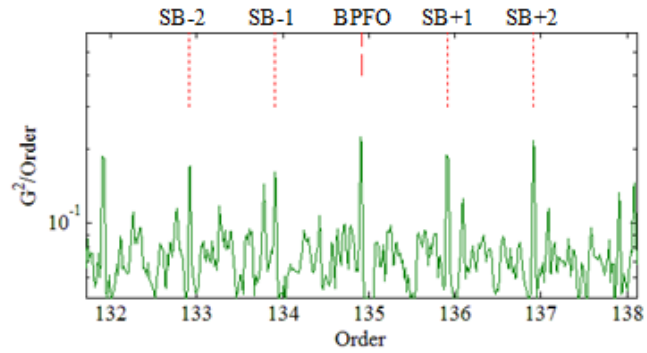

Figure 16. Measured data: Order of the envelope axial direction, third BPFO harmonic

6. CONCLUSION

This study focuses on the recognition of deformation faults in duplex ball bearings. Deformation of the bearing outer ring is a result of axial loading along with buckling of the external spacer. This study integrates the results of a 3D dynamic model, developed for assessment of the defect pattern, and results from experimental systems.

The dynamic model simulations present the defect signature as BPFO harmonics in the axial direction with adjacent shaft speed sidebands in the radial directions.

A small scale specimen was designed for preliminary results of the rings deformation. Experiments of the small scale specimen are presented in previous work (Battat at el., 2013) and are in good agreement with the model results. The full scale test rig was constructed to simulate more realistically the signals generated by the swashplate.

Experiments conducted on the test rig confirm the increase in noise sources and present the difficulty in recognizing the pattern in a realistic environment. The results present the defect pattern masked by noises, unbalance and effects of transfer function. Evident pattern can be observed in specific BPFO harmonics (e.g. the 7^{th} harmonic) in which the presence of shaft harmonics is attenuated. Use of the dephased algorithm was required in order to recognize bearing tones and their sidebands around the BPFO first harmonics. A clear bearing pattern was observed by use of envelope analysis calculated based on the dephased signal.

ACKNOWLEDGEMENT

We gratefully acknowledge the invaluable support of Dr. Avi Weinreb and Tal Yehoshua.

We would also like to thank the Perlston Foundation.

REFERENCES

Battat, M., Kogan, G., Kushnirsky, A., Klein, R., & Bortman, J. (2013). Detection of CH-53 swashplate bearing deformation-from a 3D dynamic model to diagnostics. *Proceedings of PHM Conference*. October 7-14, New Orleans, LA

Kogan, G., Bortman, J., Kushnirsky, A. & Klein, R. (2012). Ball bearing modeling for faults simulation. *The Ninth International Conference on Condition Monitoring and Machinery Failure Prevention Technologies* (no. 1, pp. 1–8).

Harris, T. A., & Kotzalas, M. N. (2007). *Essential Concepts of Bearing Technology* (Fifth Edit).USA: CRC Press.

Taylor, I. J. & Kirkland, D. W. (2004). *The Bearing Analysis Handbook*, USA: VCI

Bayoumi, A., Goodman, N., Shah, R., Roebuck, T., Jarvie, A. & Eisner, L. (2008). Conditioned-Based Maintenance at USC - Part III: Aircraft Components Mapping and Testing for CBM. *The American Helicopter Society Specialists' Meeting on Condition Based Maintenance. Huntsville*.

Klein, R., Rudyk, E., Masad, E. (2012) "Methods for diagnostics of bearings in non-stationary environment", *International Journal of Condition Monitoring*

Blechertas, V., Bayoumi, A., Goodman, N., Shah, R. & Shin, Y. J., (2009). CBM Fundamental Research at the University of South Carolina: A Systematic Approach to U.S. Army Rotorcraft CBM and the Resulting Tangible Benefits. *The American Helicopter Society Technical Specialists' Meeting on Condition Based Maintenance. Huntsville*.

Dempsey, P., Branning, J. & Arsenal, R. (2010). Comparison of Test Stand and Helicopter Oil Cooler Bearing Condition Indicators. *AHS 66th Annual Forum and Technology*.

Budynas, R. & Nisbett, K. (2006). Shigley's Mechanical Engineering Design (*Mcgraw-Hill Series in Mechanical Engineering*). McGraw-Hill Science/Engineering/Math.